Geosci. Instrum. Method. Data Syst. Discuss.,
doi:10.5194/gi-2016-15-AC2, 2016

Geoscientific Instrumentation Methods and Data Systems Discussions
Open Access
EGU

Interactive comment on "A coincidence detection system based on real-time software" *by* Sindulfo Ayuso et al.

Sindulfo Ayuso et al.

sindulfo.ayuso@edu.uah.es

Received and published: 18 July 2016

Author's response:

Thank you very much for the comments. They helped us to clarify several important issues and significantly improve the quality of our manuscript.

Please, see attached document with changes in blue.

1. (p4 l5) Authors have to justify the choice of voltage of operation based on the experimentally determined PMT response.

We agree. A new figure 2 and the following paragraph have been added in page 4.

"We can see in Fig. 2 the variation of the counter response with the bias voltage for both PMTs used in the experiment. Bearing in mind they work in coincidence coupled

to identical scintillators, we have chosen 1270 V as optimal value because it is the point where both PMTs have the same response within the plateau."

2. (p4 l14) A photo of this device is necessary

We agree. A photo has been added (new figure 3).

3. (p5 l25) This paragraph would be better understood if diagrams are used

We agree. Diagrams have been included (new figure 5).

4. (p6 l25) A full list of the physical information that may be obtained should be given.

It is difficult to make a complete list of capabilities and uses of coincidence-based systems to obtain physical information because of the large number of them. On the other hand, the reason to include this sentence in the manuscript was only to stress the importance of coincidence method giving some example of use. In order to support this claim, we have extended and referenced the initial list.

". . .may provide relevant physical information such as particle identification by the use of dE vs dE or dE vs E techniques (del Peral et al, 1995) or by means of some shielding block between pilled detectors (Chilingarian et al, 2009a); particle impact point on the detector surface (Hasebe et al, 1988) and particle energy deposition in detectors or incident direction (Karapetyan et al, 2013). Moreover, coincidence systems are used in different research areas such as medical applications, quantum physics or optics (Joost and Salomon, 2015)."

5. (p10 l1) Why?

We have added a new table (table 2) in order to justify the use of 37 GPIO.

6. (p10 l6) Figure 9 is unnecessary.

We agree. Figure 9 has been removed.

7. (p14 l17) Magnetic field rotations may only be seen when components are shown.

These do not appear in Fig 14.

Magnetic field rotation already was shown in figure 14. Please, see from bottom to top the second row. Nevertheless, the figure has been adapted to point out the magnetic field rotations by shadowing the adequate region. In addition, a new shock line and the probably location of the associated magnetic cloud have been marked in the updated figure (now, Fig. 16). The text has been slightly reworded according to the new figure.

8. (p14 l23) An estimate of the average response of both detectors and the reasons for that should be given. The decrease in the muon telescope is much faster than that of the NM. Authors must try to give an explanation for this.

We don't know what exactly the referee means with average response. We have explained at the beginning of this section that, because of CaLMa cut-off rigidity, the energy of primary CR that produce neutrons measured in CaLMa is higher than 7 GeV when protons are the primary CR. The CaLMa background count rate is 72.62 Hz. For the muon telescope, the expected energy for primary CR is higher than 10 GeV and its background count-rate is 7.66 Hz. Regarding to the second part of the referee's comment, in our opinion, what it is observed in figure 14 is just the opposite, a sharp decrease in neutron and a softer decrease in muons, as could be expected for primary cosmic rays with a higher energy threshold. Nevertheless, in order to clarify it, we have re-written the last paragraph in section 6.1.

"The good agreement between the muon and neutron data, presented in Fig. 16, validates the software-based coincidence system used to acquire the muon data. Both of them show a clear response to the passage of interplanetary disturbances. The difference in their count-rates decreases observed by both instruments in shape (faster, sharper and deeper decrease in CaLMa) and in magnitude is likely related to the different energy of the primary cosmic ray producing the secondary neutrons and muons observed at ground level, as could be expected when the primary cosmic ray energy threshold for CaLMa (neutrons mainly) is about 7 GeV and for the muon telescope is

about 10 GeV."

9. Finally, all English language mistakes have been corrected as suggested.

Author's changes in manuscript.

In order to improve the manuscript comprehension and according to the referee's advice, the following changes have been made in the original manuscript:

1. A new figure 2 has been added to clarify the bias voltage chosen for PMTs used in muon detector 1 (MD 1).

2. A new photo (figure 3) has been added showing the scintillator and the BGO in section 2.1.

3. A new figure 5 has been included in order to clarify ADC conversion process.

4. First paragraph in section 3 has been modified and four references added.

5. Table 2 has been added to justify the use of 37 GPIOs.

6. Figure 9 has been removed.

7. Figure 14 has been changed and second paragraph in page 14 has been rewritten.

8. Third paragraph in page 14 has been rewritten.

9. All suggested English language corrections have been made.

These changes will be included in final manuscript version. The final aspect can be seen in attached document. The text changes coloured in blue.

Please also note the supplement to this comment:
http://www.geosci-instrum-method-data-syst-discuss.net/gi-2016-15/gi-2016-15-AC2-supplement.pdf

Interactive comment on Geosci. Instrum. Method. Data Syst. Discuss., doi:10.5194/gi-2016-

15, 2016.

Table 2. GPIOs required by the processor card to control the ADC. We need 18 lines to read data and control one ADC. Another line is needed to enable and disable the interface buffers, which has been added to protect the processor card.

Name	*Acro.*	*# Lines*	**Description**
Data	D	13	Binary data value
Data Ready	DR	1	Active when conversion is complete.
Invalid	INV	1	Conversion error
Overflow	OVF	1	Value exceeds ULD settings
Enable Data	ED	1	Gate the 13-bit data onto the output lines
Data Accepted	DA	1	Acknowledgment of data acceptance. Reset the ADC
TOTAL lines 1 ADC		**18**	
Line to enable interface buffers		1	
TOTAL to control 2 ADCs		**37**	**18+18+1**

Fig. 1. Table 2

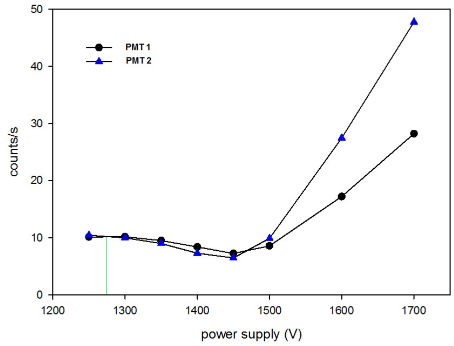

Figure 2. Counting rate versus voltage for PMTs type 53AVP (Philips). Note the plateau below 1500 V and the crossing point of both curves in 1270 V (bias voltage chosen).

Fig. 2. Figure 2

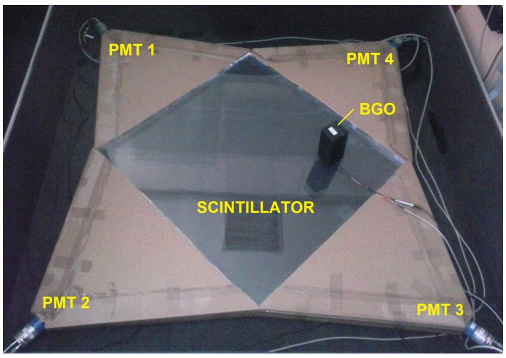

Figure 3. Main scintillator (100 cm x 100 cm x 5 cm). Four PMTs inside its pyramidal guides gather the light from lateral sides of scintillator. The BGO inside the little black box can be moved over the scintillator surface. The BGO and three PMTs work in coincidence, thus only the muon trajectories crossing the BGO will be detected and the amplitude of PMTs pulses will carry position information. The BGO is used to calibrate the system. All system is located inside a closed dark chamber.

Fig. 3. Figure 3

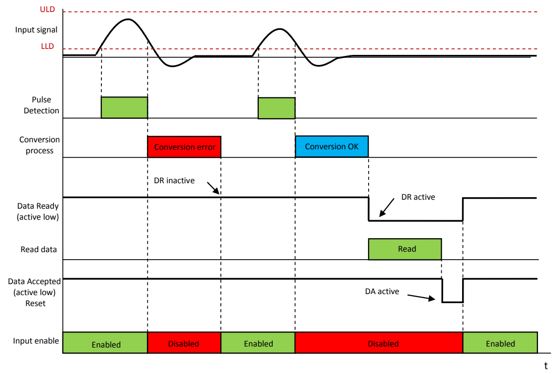

Figure 5. ADC conversion process. The ADC detects a peak when the input signal rises above the LLD threshold and below the ULD threshold. The detection process ends when the input pulse falls below 90% of its peak amplitude. In that moment, the signal input is disabled and the conversion process starts. If an error occurs in the conversion process, DR signal remains inactive and input signal enabled again. If conversion process is OK, DR is activated, the Data Acquisition System reads the data and actives DA signal, which causes the DA to go to inactive and the signal input to be enabled again.

Fig. 4. Figure 5

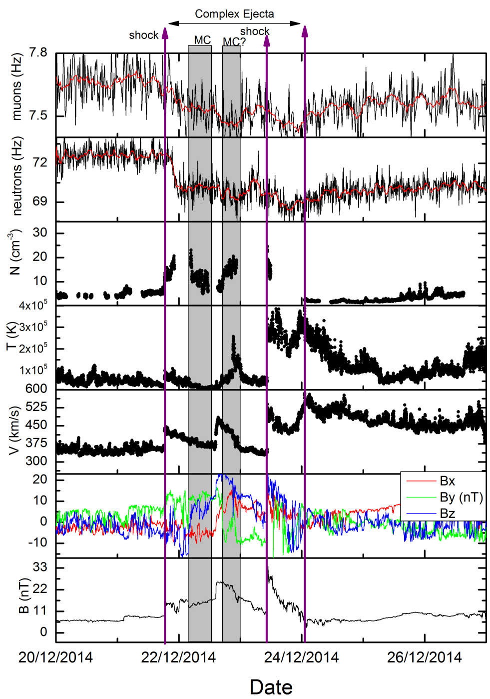

Fig. 5. Figure 16